

On the dissolution of evolving star clusters

Simon F. Portegies Zwart^{1,2}, Piet Hut³, Junichiro Makino², and Stephen L. W. McMillan⁴

¹ Astronomical Institute *Anton Pannekoek*, Kruislaan 403, 1098 SJ, Amsterdam, NL

² Department of Information Science and Graphics, College of Arts and Science, University of Tokyo, 3-8-1 Komaba, Meguro-ku, Tokyo 153, Japan

³ Institute for Advanced Study, Princeton, NJ 08540, USA

⁴ Department of Physics and Atmospheric Science, Drexel University, Philadelphia, PA 19104, USA

received; accepted:

Abstract. Using direct N-body simulations which include both the evolution of single stars and the tidal field of the parent galaxy, we study the dynamical evolution of globular clusters and rich open clusters. We compare our results with other N-body simulations and Fokker-Planck calculations. Our simulations, performed on the GRAPE-4, employ up to 32,768 stars. The results are not in agreement with Fokker-Planck models, in the sense that the lifetimes of stellar systems derived using the latter are an order of magnitude smaller than those obtained in our simulations. For our standard run, Fokker-Planck calculations obtained a lifetime of 0.28 Gyr, while our equivalent N-body calculations find ~ 4 Gyr. The principal reason for the discrepancy is that a basic assumption of the Fokker-Planck approach is not valid for typical cluster parameters. The stellar evolution timescale is comparable to the dynamical timescale, and therefore the assumption of dynamical equilibrium leads to an overestimate of the dynamical effects of mass loss. Our results suggest that the region in parameter space for which Fokker-Planck studies of globular cluster evolution, including the effects of both stellar evolution and the galactic tidal field, are valid might be rather small.

Key words: methods: numerical – celestial mechanics: stellar dynamics – stars: evolution – globular clusters: general – open clusters and associations: general

1. Introduction

Theoretical models for the evolution of star clusters are generally too idealized for comparison with observations. However, detailed model calculations with direct N-body

Send offprint requests to: Simon Portegies Zwart: spz@grape.c.u-tokyo.ac.jp

* Japan Society for the Promotion of Science Fellow

methods are not feasible for real globular clusters, even with fast special-purpose computers such as GRAPE-4 (Makino et al. 1997) or advanced parallel computers (Spurzem and Aarseth 1996).

If we could scale the results of N-body simulations with relatively small numbers of particles (such as $\sim 30,000$) to real globular clusters, then it would become feasible to perform computations with relatively small numbers of particles and still derive useful qualitative conclusions about larger, more massive systems. However, to determine the proper scaling is difficult because the ratio between two fundamental time scales, the relaxation times and the dynamical time, is proportional to N . In typical globular clusters, this ratio exceeds 10^3 and the two time scales are well separated. In N-body simulations, the ratio is generally much smaller.

The inclusion of realistic effects such as mass loss due to stellar evolution and the effect of galactic tidal fields (with the galaxy approximated as a point mass, but also with the inclusion of disc shocking) further complicate the scaling problem (see, e.g., Heggie 1996). A proper treatment of stellar evolution is particularly problematic, since its characteristic timescale changes as stars evolve.

Chernoff & Weinberg (1990, CW90) performed an extensive study of the survival of star clusters using Fokker-Planck calculations which included 2-body relaxation and some rudimentary form of mass loss from the evolving stellar population. In their simulations the number of particles is not specified. Their models are defined by the initial half-mass relaxation time and by the initial mass function of the cluster. Since their models do not specify the number of stars per cluster, each of their model calculations corresponds to a one-dimensional series of models, when plotted in a plane of observational values, such as total mass versus distance to the galactic center (fig. 1). All points of the solid line in that figure correspond to a single calculations by CW90, since they have an identical relaxation time. As we will see later, it is useful to con-

sider other series of models, for which the crossing time is held constant while varying the mass. An example of such a series is indicated by the dashed line in fig. 1. The shapes of these lines are derived under the assumption of a flat rotation curve for the parent galaxy.

The main conclusion of CW90 was that the majority of the simulated star clusters dissolve in the tidal field of the galaxy within a few hundred million years. Fukushige and Heggie (1995, FH95) studied the evolution of globular clusters using direct N -body simulation, using the same stellar evolution model as used by CW90. They used a maximum of 16k particles and a scaling in which the dynamical timescale of the simulated cluster was the same as that of a typical globular cluster, corresponding to one of vertical lines in fig. 1.

FH95 found lifetimes much longer than those in CW90's Fokker-Planck calculations, for the majority of the models used in CW90. However, the reason for the discrepancy is rather unclear, because the calculations of FH95 and those of CW90 differ in several important respects. The relaxation times differ because FH95 held the cluster crossing time fixed in scaling from the model to the real system. However, the crossing times themselves are also different, since the crossing time is by definition zero in a Fokker-Planck calculation. Finally, the implementation of the galactic tidal field is also quite different. CW90 used a simple boundary condition in energy space (spherically symmetric in physical space), in which stars were removed once they acquired positive energy, but the underlying equations of motion included no tidal term. FH95 adopted a much more physically correct treatment, including tidal acceleration terms in the stellar equations of motion and a proper treatment of centrifugal and coriolis forces in the cluster's rotating frame of reference (see FH95).

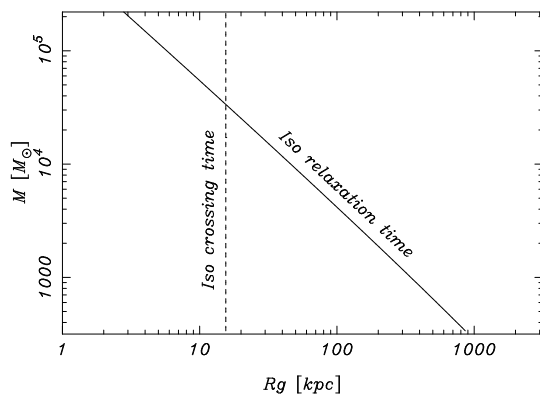


Fig. 1. Cluster mass versus the distance to the galactic center. The solid line indicates the model parameters for which the relaxation time is constant (iso relaxation time); the dashed line indicates the initial conditions for which the crossing time of the star cluster is constant (iso crossing time)

In order to study the behavior of star clusters with limited numbers of stars, and to compare with the results of the Fokker-Planck simulations of CW90, we perform an equivalent series of collisional N -body simulations in which the evolution of the individual stars is taken into account. We find that Fokker-Planck models do not provide a qualitatively correct picture of the evolution of star clusters. The effects of the finite dynamical time scale are large, even for models whose lifetime is several hundred times longer than the dynamical time.

The main purpose of this paper is to study the survival probabilities of star clusters containing up to a few tens of thousands of single stars, in order to gain a deeper understanding of the influence of the galactic tidal field and the fundamental scaling of small N clusters to larger systems. Only single stars are followed; primordial binaries are not included. The computation of gravitational forces is performed using the GRAPE-4 (GRAvity PipE, see Ebisuzaki et al. 1993, a special-purpose computer for the integration of large collisional N -body systems). Hardware limitations (speed as well as storage) restrict our studies to less than ~ 32 k particles.

The dynamical model, stellar evolution, initial conditions and scaling are discussed in sect. 2. Section 3 reviews the software environment and the GRAPE-4 hardware, and discusses the numerical methods used. The results are presented in sect. 4 and discussed in sect. 5; sect. 6 sums up.

2. The model

The simulations presented in this paper were performed by a computer code that consists of two independent parts. One part, the N -body model, integrates the equations of motion of all individual stars while the other part computes the evolution of each single star (see sect. 3 for a description of the numerical implementation).

2.1. Stellar dynamics

The equations of motion of the stars in the stellar system are computed using Newtonian gravity. The numerical integration is performed using a fourth-order individual-time-step Hermite scheme (Makino and Aarseth 1992; see sect. 3 below).

The radius of the star cluster is limited by the galactic tidal field. We assume for simplicity that the cluster describes a circular orbit around the galactic center. At fixed time intervals, stars that are outside the tidal radius are simply removed. We chose this simple cutoff in order to facilitate direct comparison with the Fokker-Planck results. Shocks due to the passage of the cluster through the galactic plane, twice per orbit, and encounters with giant molecular clouds are neglected.

At regular time intervals, the stellar evolution model updates all stars to the current age of the stellar system

and the N -body model is notified of the changes in mass and radius of the stars. Whenever a star loses more than 1% of its mass, the dynamical part of the simulation is reinitialized, to take into account the loss of mass and energy from the system. A treatment of collisions and mergers involving two or more stars is also included.

2.2. Stellar evolution

The evolution of single stars in our model is performed using the stellar evolution model presented by Portegies Zwart & Verbunt 1996, and later dubbed *SeBa* (see Portegies Zwart et al. 1997ab for a dynamical implementation). These models are based on fitting formulae to stellar evolution tracks of population I stars given by Eggleton et al. (1989) (evolutionary tracks for population II stars are not yet available in this convenient form). These equations give a star's luminosity and temperature as functions of age and initial mass. Other stellar parameters—radius, mass loss and the mass of the core—are then from these.

We point out here a few important details of the evolutionary model: A star with a mass larger than $8 M_{\odot}$ becomes a neutron star in a supernova, less massive stars become white dwarfs. Neutron stars have a mass of $1.34 M_{\odot}$; the mass of a white dwarf is given by the core of the star as it leaves the end of the supergiant branch.

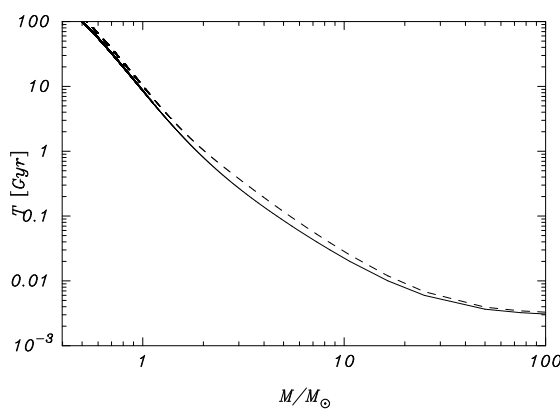


Fig. 2. Main-sequence lifetime (solid line) and terminal age (dashed line) in billions of years for stars as a function of the zero age mass of the stellar evolution tracks of Eggleton et al. (1989).

Mass lost by stellar evolution, either in the form of a stellar wind or after a supernova, escapes from the stellar system, as the velocity of the stellar wind or supernova shell exceeds the escape velocity of the star cluster. The escaping mass is presumed to carry away the same specific energy and orbital angular momentum as the mass-losing star has.

2.3. Initial conditions

For the initial model, we followed the specifications of CW90. Each simulation is started at $t = 0$ by giving all stars a mass m drawn from a single-component power-law mass function of the form $dN(m) = m^{-\alpha} dm$, between lower and upper mass limits m_- and m_+ , respectively. From the mean mass $\langle m \rangle$, given by the mass function, and the total number of stars in the computation N , the initial mass of the star cluster is computed: $M = N\langle m \rangle$.

The initial density profile and the velocity distribution of the stellar system are taken from King models (King 1966). In a King model, the dimensionless depth of the central potential W_0 determines the structure of the cluster and thus the ratio of the virial radius r_{vir} to the tidal radius r_t (see e.g. Binney & Tremaine 1987). The velocity distribution is given by a lowered Maxwellian with the same formal velocity dispersion for all stars, independent of mass. The initial positions of the stars are chosen independent of their mass.

The tidal radius is computed assuming that the star cluster initially fills its Roche lobe in the tidal field of the galaxy. In other words, we take the tidal radius of the initial King model as the physical tidal cutoff radius (Takahashi et al. (1997)). The mass of the galaxy M_G and distance R_G from the cluster to the center of the galaxy are related by assuming that the star cluster has a circular orbit around the galactic center with a velocity of $v_G = 220 \text{ km s}^{-1}$:

$$M_G(R_G) = \frac{v_G^2 R_G}{G}. \quad (1)$$

We approximate the tidal radius r_t as the Jacobi radius for the star cluster. The distance from its center of mass to the first Lagrangian point is:

$$r_t(R_G) = \left(\frac{M}{3M_G} \right)^{1/3} R_G. \quad (2)$$

After each diagnostic output, the new tidal boundary of the star cluster is determined, stars outside the tidal boundary are removed from the stellar system. As in CW90, no tidal force is applied to the individual members of the star cluster. The mass of the star cluster declines during its evolution due to mass loss from stellar evolution of the stars and from escaping stars; the tidal radius decreases accordingly.

All our model clusters start in virial equilibrium.

2.4. System of units

The system of units used in the N -body model are given by $M = G = -4E = 1$, where E is the initial internal energy of the stellar system (Heggie & Mathieu 1986). The transformation from these scaled N -body units to physical units is realized with a set of transformations for mass, length and time.

The total mass of the stellar system determines the mass scaling. Since the star cluster starts filling its Roche lobe, the size scaling is determined by the tidal radius of the initial King model, which is in turn set by the tidal radius of the star cluster in the galactic tidal field. In this paper, we have adopted as the definition of the half-mass crossing time a time of order unity in our natural system of units (Heggie & Mathieu 1986). This corresponds to

$$t_{hc} = 15 \left(\frac{[M_{\odot}]}{M} \right)^{1/2} \left(\frac{r_{\text{vir}}}{[\text{pc}]} \right)^{3/2} [\text{Myr}]. \quad (3)$$

Here r_{vir} is the virial radius of the stellar system. Note that $r_{\text{vir}} = 1$ is our standard units, whereas the relation between r_{vir} and r_t is determined by the King parameter W_0 .

3. Numerical method and its validation

3.1. Software

For all runs, we used the integration program `kira` in the Starlab software toolset (McMillan & Hut 1996). Starlab is a collection of utility programs developed for numerical simulation of star clusters and the data analysis of the results of the simulation. Utility programs in Starlab are divided into four classes: (a) programs which create N -body snapshots, (b) programs which apply some transformation to N -body snapshots, (c) programs which perform time integration, and (d) programs which analyze N -body snapshots. The I/O interface of all of these programs is unified in such a way that the output of one program can always be used as the input for another program through the UNIX pipe mechanism.

The integration program `kira` performs the online analysis needed in this work. The time integration scheme used in `kira` is the individual timestep with a 4th-order Hermite scheme (Makino and Aarseth 1992), which is essentially the same as the one used in Aarseth's NBODY4 and NBODY6. What sets `kira` apart from these other programs is the way it handles close encounters and compact subsystems. In NBODYx, the subsystems are handled by various regularization techniques according to the number of particles and their dynamical states. In contrast, `kira` models any compact subsystem as a local hierarchical binary tree. This procedure provides a great algorithmic simplification, without significant loss in either accuracy or speed.

Another difference between `kira` and the older NBODYx codes concerns the data structures used. `kira` is written in an object-oriented style in which each star is an object with properties which represent the dynamics (mass in dynamical units, position, velocity etc.) and properties which represent the stellar evolution (mass in solar masses, age, effective temperature, luminosity, state of the star, chemical composition and so on). The part of the code which handles the dynamics and the part that

handles the stellar evolution are completely independent of each other. The communication between the two parts can take place only locally, for one individual star at a time, and only at one well-defined point in the code, where the dynamical and evolutionary information of that star are allowed to exchange information. This design makes it possible to combine complex N -body integration programs and complex stellar evolution packages without major problems in either compatibility or maintenance.

Currently, the stellar evolution is handled in the following way. At a pre-specified time interval, the diagnostic time step (see fig. 3), the stellar evolution package `SeBa` is called for all stars in the system and the mass and state of the stars are updated. If the change of the mass of any star exceeds a prescribed limit, the mass of all stars used in the N -body integrator is updated, the energy change due to that change is calculated, and the integrator is re-initialized.

Since we invoke stellar evolution and tidal truncation only at fixed time intervals, the results of the calculation might conceivably depend on the specific time interval used. We discuss this possibility below, in section 3.3. 1.

3.2. The hardware

The time integration in `kira` for this study is performed using the special purpose computer GRAPE-4 (Makino et al. 1997). GRAPE-4 is an attached processor which calculates the gravitational interactions between stars. The actual time integration is done on the host computer, which runs the UNIX operating system. Starlab programs and packages all reside on the host computer.

The peak speed of the fully configured GRAPE-4 system is 1.08 Tflops. For this study, we mostly use the smallest configuration with a peak speed of 30 Gflops.

3.3. Test of the method

In this section, we describe the result of the test runs in which we varied the time intervals to invoke the stellar evolution package and tidal removal of stars. As we mentioned above, this choice could have a large effect, in particular at the early stage where the high-mass stars, which evolve very quickly, dominate the evolution of the stellar system.

We performed the simulation from the same initial conditions for 1024- and 4096-body systems, changing the time interval to invoke the mass loss due to stellar evolution from 1/256 to 4. The time interval to remove the stars out of the tidal radius is taken to be the same as the time interval for stellar mass loss. In these runs, all runs resulted in the evaporation of the cluster in less than 100 Myrs. Table 1 and Fig. 3 give overviews of the results.

If the stellar evolution time interval is taken to be larger than the crossing time, then the lifetime of the stellar system is extended considerably. On the other hand,

as long as the evolution time step is taken to be a small fraction of the crossing time, its precise choice of value has a relatively small effect on the lifetime of the cluster and run-to-run variations due to small number statistics are larger than any systematic effects caused by the choice of time interval.

In these models, the crossing time corresponds to 1.7 Myr. If the diagnostic time interval is chosen to be longer than the crossing time, it would exceed the lifetime of the most massive stars. This in turn would delay the effects of stellar evolution to be felt dynamically, which would artificially extend the lifetime of the cluster. This effect is illustrated in fig. 3.

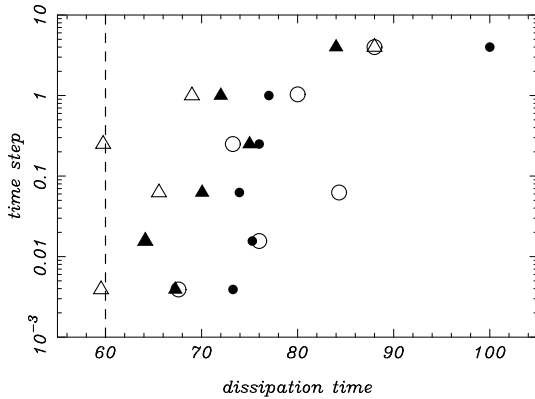


Fig. 3. Life time of the star clusters from the test runs with 1k (triangles) and 4k (circles) stars (see Tab. 1) as a function of the diagnostic integration time step (both in units of the initial crossing time of the stellar system). The filled symbols refer to the computations with the same initialization, open symbols are from different random initializations. The vertical dashed line indicates the result from FH95 for a run with 8k stars.

We performed a second set of test runs using the same initial conditions as one of the runs in FH95 (the run shown in their figure 7). The results of our test runs is given in Tab. 2. There are two reasons to perform this test, namely to investigate the effect of the rather large softening used by FH95, and to evaluate to what extent different treatments of a tidal limit influence the value of the final dissipation time.

Figure 4 demonstrates that the evolution of the total mass is qualitatively different for runs with less than 16k particles and the run with 16k particle. In FH95, this transition took place around $N = 4096$. This result is quite natural since the relaxation effect is 2-3 times smaller in the FH95 runs, because of the large softening.

Our cluster dissolution times turn out to be roughly a factor of two longer than those reported by of FH95. There are two reasons for this discrepancy, as can be read from Figure 5. One reason is the fact that we do not use anything softening in our production runs. Adding a softening, comparable to that used by FH95, cuts our dissolu-

Table 1. Series of test runs with 1k and 4k particles of star clusters with the following initial conditions $W_\odot = 3$, $\alpha = 1.5$ between 0.4 and $14M_\odot$ and $r_{\text{vir}} = 3.2$ pc and $r_{\text{vir}} = 5.1$ pc for the runs with 1k and 4k stars, respectively (where we keep the crossing time fixed, at ~ 1.7 Myr). The numbers in the table are in units of the N -body time. The first column gives the name of each test model. The second column gives the diagnostic time step for synchronization of the dynamical integrator and the stellar evolution part of the code. The next two columns give the time (in units of a N -body time) in which the 1k models dissolve, followed by two columns that display the time in which the 4k models dissolve. The columns listed as “1k” and “4k” refer to calculations in which the exact same initial conditions were used throughout a single column. The columns listed with an extre “(r)” refer to calculations for which each run was started from a new, random realization.

model	dt	1k	1k(r)	4k	4k(r)
T1	1/256	67	60	73	68
T2	1/64	64	64	75	76
T3	1/16	70	66	74	84
T4	1/4	75	60	76	73
T5	1	72	69	77	80
T6	4	84	88	100	88

Table 2. The computations in which we attempt to reproduce the results from FH95 are based on a star cluster of family 1 (see CW90), with a total mass of $1.49 \cdot 10^5 M_\odot$. The mass function is given by $\alpha = 2.5$ between $0.4M_\odot$ and $14M_\odot$ and $W_\odot = 3$. The crossing time is about 1.9 Myr and the distance to the galactic center is about 4 kpc. The first column gives the model name, followed by the number of particles in the simulation, the tidal radius, the virial radius, and the time for dissolving the system in the tidal field of the galaxy in crossing times and in billion years.

model	N	r_t [pc]	r_{vir} [pc]	t_{diss} [t_{hc}]	t_{diss} [Gyr]
FH1	1k	8.0	2.58	220	0.42
FH2	2k	10.1	3.31	420	0.83
FH4	4k	12.7	4.02	690	1.3
FH8	8k	16.0	5.12	1000	1.9
FH16	16k	20.1	6.36	1100	2.0

tion time roughly in half. Another reason stems from the difference in treatment of tidal limitations of the model cluster. Our choice of a simple tidal cutoff, rather than the more elaborate and physically correct tidal field employed by FH95, effectively weakens the tidal effect in our calculations, increasing the cluster lifetime.

Figure 5 compares several realizations of run FH8 (Table 2), some using our simple spherical cutoff, others with a tidal field equivalent to that employed by FH95. All runs were performed using `kira`. When both changes are made, adding a large softening as well as a more accurate treat-

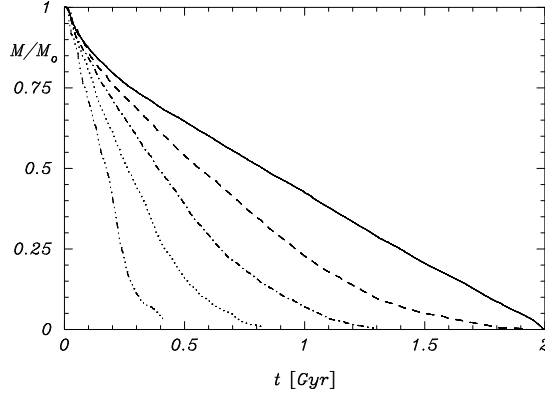


Fig. 4. The time evolution of the total mass of the models FH1 (dash-3dot line), FH2 (dotted), FH4 (dash dot), FH8 (dashed line) and FH16 (solid line).

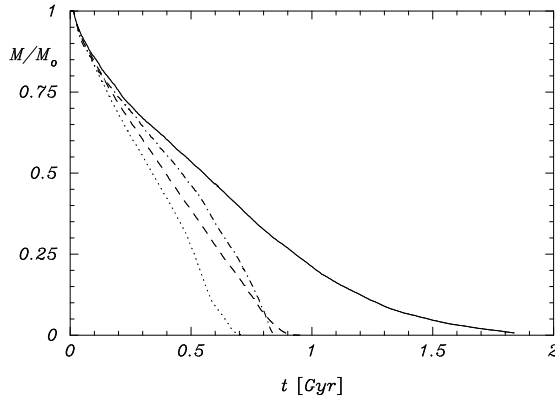


Fig. 5. The time evolution of the total mass for models similar to model FH8 but with various choices for the tidal field and softening. The solid line gives the results of model FH8 with a tidal cut off and without any softening (similar to the dashed line in Fig. 4). The dashed line gives the result for the more elaborate implementation of the tidal field (no softening). The dash-dotted and the dotted line give the results for the softened models with a tidal cut-off and with the tidal field, respectively. For each line the average of two runs with identical initial conditions are selected (with a typical run-to-run variation of lifetimes of only a few percent).

ment of the tidal field (dotted line), the dissolution time diminishes even further, to less than 40% of that of our normal run (solid line).

FH95's treatment of the tidal field is physically correct, but it complicates comparison of the N -body results with the CW90's Fokker-Planck results. For that reason, in the remainder of this comparative paper, we continue to use a simple tidal cutoff. However, the reader should note that the dissolution times reported below are probably too long by a factor of two.

3.4. Initial IC and IR models

We consider the King model with $W_0 = 3$ with an initial half-mass relaxation time of 2.87 billion years (family 1 of CW90) as our standard model. (Note here that the relaxation time used by CW90 is defined at the tidal radius of the star cluster instead of at the virial radius.) The slope of the initial mass function is fixed to $\alpha = 2.5$. The cutoff values of the mass distribution at high- and low-mass end are taken as $14 M_\odot$ and $0.4 M_\odot$, respectively. These values are chosen so that they are the same as the parameters used in CW90. (Note that CW90 quote both $14 M_\odot$ and $15 M_\odot$ as upper limits for their initial mass function.)

The number of particles we used for the standard model is 32768. Tab. 3 summarizes the characteristics of the standard model.

Starting from the standard model, we generated two series of initial models. We designed the first series of runs (referred to below as iso-relaxation, or IR, models) so that our N -body results can be directly compared with the Fokker-Planck calculation of CW90. All parameters are chosen to be the same as used by those authors. Models of this series have the same initial half-mass relaxation time, and therefore all belong to CW90's family 1. The only difference is that our models are N -body systems with finite crossing time and a fully 6-dimensional phase-space distribution of particles, while CW90 used Fokker-Planck calculations with infinitesimal crossing time and one-dimensional distribution function. CW90 obtained a lifetime of 280Myr for this particular model. This first sequence is shown as thick solid line in figure 6.

Models in the second series (iso-crossing, or IC, models) have the same initial half-mass crossing time; these are similar to the runs described by FH95. This sequence is shown as thick dashed line in figure 6.

4. Results

4.1. Model S: the standard model

In this section we describe the result of the standard run with 32768 particles.

Table 3. Initial conditions and resulting dissolution time of the main model with 32k stars. The first column gives the name of the model followed by the number of stars, the tidal radius and the virial radius (both in parsecs), the crossing time of the virial radius in million years and the relaxation time (in billions of years). The last two columns contain the dissolution time in units of the half-mass crossing time and in billions of years.

model	N	r_t [pc]	r_v [pc]	t_{hc} [Myr]	t_{rlx} [Gyr]	t_{diss} [t_{hc}]	t_{diss} [Gyr]
S	32k	62.5	19.94	7.29	2.87	520	3.8

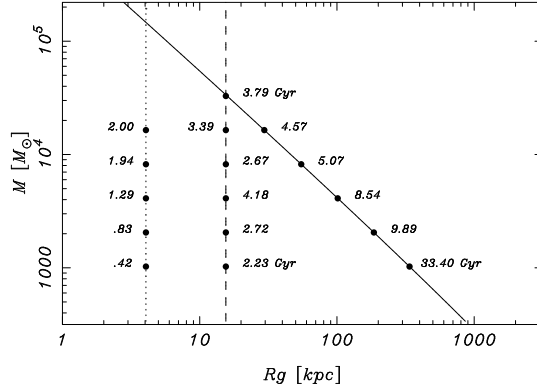


Fig. 6. The mass of the models plotted versus the distance to the galactic center. The filled circles indicate the simulated models with the life time of the model in billion years next to the symbol. The solid line gives the iso relaxation time models which are comparable to Chernoff & Weinberg's family 1, the dashed line gives the iso crossing time models. The dotted lines give the iso relaxation time models of the other families (2, 3, and 4) of CW90.

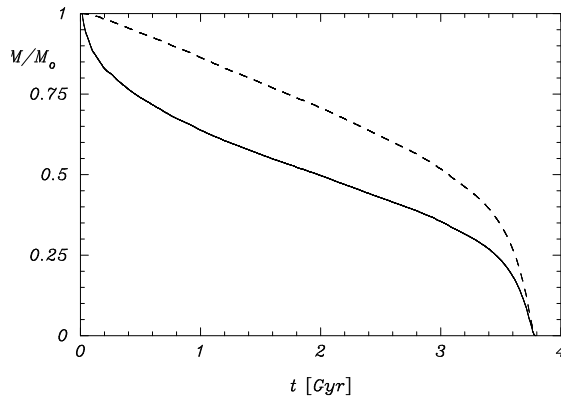


Fig. 7. The time evolution of the total mass (solid line) and number of stars (dashed line) of the cluster for the standard, 32768-body run. Both the mass and the number of stars are normalized to their initial value.

Figure 7 gives as a function of time (in billions of years) the total mass and the total number of stars of the simulation model S. This figure clearly demonstrates the initial epoch of quick mass loss due to stellar evolution followed by a gradual decrease in the total number of stars. Finally the stellar system evaporates.

4.2. Models IR: constant relaxation time

Tab. 4 and figure 8 give the results of the series of runs with constant relaxation time.

A striking feature of figure 8 is the systematic way in which lifetimes are shorter for models with larger total mass. This trend can be explained as follows. For lower

Table 4. Initial conditions and dissolution time in the galactic tidal field for the models with constant relaxation time. The columns give the model name, the number of particles, the tidal and the virial radius (in parsec) and the half mass crossing time in million years. The last two columns gives the life time of the star cluster in units of the half mass crossing time and in billion years. The relaxation time scale at the virial radius of these model is approximately 2.87 Gyr

model	N	r_t [pc]	r_v [pc]	t_{hc} [Myr]	t_{diss} [t_{hc}]	t_{diss} [Gyr]
IR1	1k	151	47.5	151.8	220	33
IR2	2k	128	40.5	84.5	120	9.9
IR4	4k	108	34.8	47.5	180	8.5
IR8	8k	90.1	28.1	24.4	210	5.1
IR16	16k	75.2	24.2	13.8	330	4.6

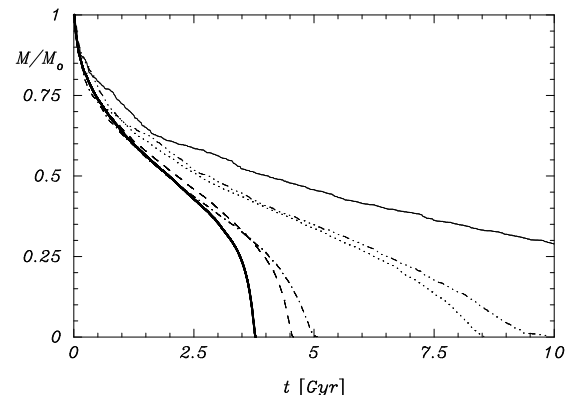


Fig. 8. The mass of the star cluster as a function of time for the runs with constant relaxation time (models IR) of the models with 32k (left solid line), 16k (dashed), 8k (dash-dot), 4k (dotted), 2k (dash-3dot) and 1k (right solid line) runs. The time scaling is cut off at 10 Gyr, at which point model IR1 has still not dissolved completely.

mass models, holding the relaxation time fixed implies that the crossing times are longer. Since stars can escape from the system only on a crossing timescale at the tidal boundary, an increase in crossing time tends to increase the dissolution time. In addition, effects of stellar evolution make themselves felt only on a crossing time, which again tends to lengthen the dissolution time for lower mass models.

The latter effect is most notable during the first $\sim 10^8$ years, when the mass of the stellar system decreases dramatically. This initial mass decrease is the result of the presence of massive stars which evolve quickly. After the system has lost about 20% of its initial mass escaping stars become the major channel through which mass is lost until the system dissolves.

By the time half of the mass has been lost, these above arguments, related to the length of the crossing time, become less important, since the time scale for significant

change to take place has become longer. The subsequent difference in behavior is linked to the onset of an instability, noted already by FH95, that operates only for high number of stars, where an increase of the ratio r_{vir}/r_t leads to a loss of virial equilibrium, and a consequent rapid dissolution of the cluster.

The strong dependence of the dissolution time on the crossing time implies that we cannot easily extrapolate the result obtained from small- N runs to the evolution of globular clusters with realistic number of particles. From figure 8, it is not clear whether or not the lifetime is converging to a particular value. One would hope that, in the limit of $N \rightarrow \infty$, the result would converge to the result of the Fokker-Planck calculation. Even so, we have to face the question whether real globular clusters contain a large enough number of stars to be modeled by Fokker-Planck calculations. So far, we have used up to 32,768 particles, a vastly larger number than any previous N -body simulations intended to model globular clusters. The separation between the relaxation timescale and the crossing timescale is quite large (more than two orders of magnitude), and the lifetime of the system is measured in hundreds of the crossing times. Even so, we still see a fairly strong dependence on the crossing time for the evolution timescale of the total cluster.

In the next subsection, we examine the other way to adjust the timescales, in the series of models with constant crossing times.

4.3. Models IC: constant crossing time

Table 5 and figure 9 shows the result of the runs with constant crossing time. Here, the models with $N \leq 4096$ and those with $N \geq 8192$ behave differently, in the sense that the latter models show quick disruption at the end, while the former models do not. Within the models which show the same qualitative behavior, models with longer relaxation time evolve more slowly.

It is natural that systems with shorter relaxation times evolve faster. If the effect of the stellar evolution is not dominant, the main mechanism which drives the evolution of the cluster is two-body relaxation. Thus, the evolution timescale is determined by the relaxation timescale.

5. Discussion

Chernoff & Weinberg obtained a lifetime of 280 Myr for stellar systems with a relaxation time as is chosen in the models S and IR1 to IR16. None of our models disrupts within such a short time span, but the trend of shorter life time for larger mass cluster is clearly visible. However, it seems somewhat unlikely that real globular clusters could have a disruption time of a few hundred Myrs, if we extrapolate our numerical result. The largest number of particles used in our calculations already reaches within a factor of 10 of that of the smaller globular clusters.

Table 5. Initial conditions and resulting lifetimes of model clusters where the stellar evolution time is scaled to the half-mass crossing time of model S ($t_{hc} = 7.31\text{Myr}$). The first two columns gives the model name and number of stars. The third and fourth columns give the initial tidal radius and virial radius in parsec followed by the relaxation time (in billion years). The last two columns give the dissipation time scale in units of the initial half mass crossing time and in billion years.

model	N	r_t [pc]	r_v [pc]	t_{rel} [Myr]	t_{diss} $[t_{hc}]$	$[{\text{Gyr}}]$
IC1	1k	19.69	6.51	142	290	2.2
IC2	2k	24.80	8.02	250	370	2.7
IC4	4k	31.28	9.99	450	570	4.2
IC5	5k	33.18	10.7	544	570	4.2
IC6	6k	35.26	11.4	641	650	4.7
IC7	7k	37.23	12.1	740	430	3.2
IC8	8k	39.40	12.7	843	360	2.7
IC16	16k	49.63	15.6	1510	460	3.4

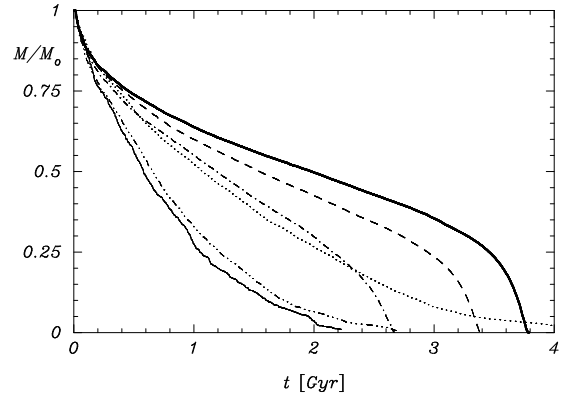


Fig. 9. Mass (normalized to unity) as a function of time (in billion years) for the computations of model IC1 (lower solid line) to IC32 (upper solid line). Line styles are the same as in fig. 8. The lines for the models IC5 to IC7 are not presented in this figure. Note the different scale along the time axis compared to fig. 8.

As we stated earlier, this rather large discrepancy between the result of our N -body calculation and the result of the Fokker-Planck calculation is surprising. There are several reasons which would cause the evaporation of the Fokker-Planck model to be different from that of N -body system. For example, the Fokker-Planck calculation relies on the assumption of the adiabatic response of the orbits of stars to a change of mass of the stars, assumed to be slow. This assumption is violated for the early stage of evolution, where the stellar evolution time scales are as short as a few Myr.

Another difference is that, in Fokker-Planck calculations, a simple tidal limit value in energy space is used; stars with energy exceeding this value disappear from the

cluster. In our study, we remove stars when they reach the tidal radius. Apart from the fact that these two procedures are already different, neither of them are appropriate. In the Fokker-Planck calculation, both the anisotropy and the nonspherical nature of the system, both which might have the effect of significantly enhancing the stellar escape rate, are ignored. Our simple treatment of the tidal boundary allows direct comparison with CW90, but it also has the effect of reducing the escape rate, as no external tidal force is applied to individual stars. This is the main reason why our test models obtained significantly longer life times than those obtained by FH95.

In order to investigate the reason for the discrepancy between different models, both the N -body calculation and Fokker-Planck calculation have to be refined. On the side of the Fokker-Planck calculation, until recently, further refinement has been difficult, since no practical implementation for anisotropic models was available. However, recent progress in the two-dimensional Fokker-Planck calculation code (Takahashi 1993, 1995, 1996) has made the study of the effects of anisotropy feasible.

On the N -body side, it is fairly straightforward to try various models for the tidal field, from the simplest one used in our present study to the realistic static model used in FH95 (see Fig. 4). It is even possible to go further to include the dynamic effects of the galactic disk and the bulge. Thus, a more detailed comparison may be possible (see the fascinating “collaborative experiment” reported by Heggie 1997).

However, even if the N -body and Fokker-Planck calculations treat the tidal boundary and the anisotropy in the same way, the difference in the dynamical timescale still remains. For the next several years, we will not yet be able to model real globular clusters accurately, since they will continue to fall in between the Fokker-Planck calculations (with an infinitesimal crossing time) and N -body calculations (with too long a crossing time). We thus urgently need some way to interpolate between the two types of results.

The main purpose of the present study is to investigate whether such an extrapolation is feasible. We must conclude that, as yet, there is no obvious way to extrapolate the results from small N values upward. The models with constant relaxation time evolve too slowly, because the crossing time is unphysically long. The models with constant crossing time, on the other hand, evolve too rapidly, because the relaxation timescale is too short. Although we knew these two effects to be qualitatively present, it came to us as a bit of a surprise to see just how important they are, quantitatively.

Consequently, it would be practically impossible to predict the result of a 32k run, from either of the 4k runs, the one from the IC series, as well as the one from the IR series. Even having both in hand would make an extrapolation still dubious. This suggests that an extrapolation

to real globular clusters, with hundreds of thousands of stars, is still out of the question.

6. Conclusions

We have followed the evolution of a star cluster, to the point of dissolution in the tidal field of the parent galaxy, taking into account both the effects of stellar dynamics and of stellar evolution. Our calculations are based on direct N -body integration, coupled to approximate treatments of stellar evolution.

Our results differ greatly from those obtained with Fokker-Planck calculations, as presented by CW90: their model clusters dissolve after a few times 10^8 years, whereas our equivalent model clusters live at least ten times longer. As we discussed in the previous section, a number of different reason conspire to produce such a drastic difference.

Our hope was that we would be able to find a way to bridge our N -body results and previous results based on Fokker-Planck approximations. The fact that the GRAPE-4 special-purpose hardware allowed us to model much larger numbers of particles, reaching to within an order of magnitude of that of real globular clusters, seemed to indicate that it would finally be possible to make a firm connection between the two types of simulations. However, our results indicate that no clear process of extrapolation has emerged yet. Even within the different runs we have studied, extrapolation from the smaller to the larger number of stars would have resulted in rather large errors. This suggests that further extrapolation will suffer from the same fate.

In the present paper, we have studied in detail a single model. However, the way the result depends on the time scaling might be different for other models. In a subsequent paper, we plan to carry out a systematic study, similar to the one we have presented here, for a much wider range of initial models.

Acknowledgements. We would like to thank Peter Eggleton, Douglas Heggie, Tijn Smit and Koji Takahashi for many stimulating discussions. This work was supported in part by the Netherlands Organization for Scientific Research (NWO) under grant PGS 78-277 and SIR 13-4109 and by the Leids Kerkhoven Boscha Fonds. SPZ thanks the Institute for Advanced Study and the University of Tokyo for their hospitality. Edward P.J. van den Heuvel of the Astronomical Institute “Anton Pannekoek” is acknowledged for financial support and for inviting our group for an extended work visit. This investigation is supported by Spinoza grant 08-0 to E. P. J. van den Heuvel.

References

- Binney, J., Tremain, S. 1987, Galactic Dynamics, Princeton series in Astrophysics, Princeton
- Chernoff, D., Weinberg, M. 1990, ApJ, 351, 121

Ebisuzaki, T., Makino, J., Fukushige, T., Taiji, M., Sugimoto, d., Ito, t., Okumura, S. K. 1993, *Publ. Astr. Soc. Japan*, 45, 269

Eggleton, P., Fitchett, M., Tout, C. 1989, *ApJ*, 347, 998

Fukushige, T., Heggie, D. C. 1995, *mnras*, 276, 206

Heggie, D. C. 1996, in P. Hut, J. Makino (eds.), *IAU Symposium 174*, Kluwer, Dordrecht, 131

Heggie, D. C. 1997, in *IAU Joint Discussion 15*, Kluwer, Dordrecht, in preparation

Heggie, D. C., Mathieu, R. 1986, in P. Hut, S. McMillan (eds.), *Lecture Not. Phys* 267, Springer-Verlag, Berlin, 233

King, I. R. 1966, *AJ*, 71, 64

Makino, J., Aarseth, S. J. 1992, *Publ. Astr. Soc. Japan*, 44, 141

Makino, J., Taiji, M., Ebisuzaki, T., Sugimoto, D. 1997, *ApJ*, 480, 432

McMillan, S. L. W., Hut, P. 1996, *ApJ*, 467, 348

Portegies Zwart, S. F., Hut, P., McMillan, S. L. W., Verbunt, F. 1997, *A&A*, 328, 134

Portegies Zwart, S. F., Hut, P., Verbunt, F. 1996, *A&A*, 328, 130

Portegies Zwart, S. F., Verbunt, F. 1996, *A&A*, 309, 179

Spurzem, R., Aarseth, S. J. 1996, *MNRAS*, 282, 19

Takahashi, K. 1993, *Publ. Astr. Soc. Japan*, 45, 789

Takahashi, K. 1995, *Publ. Astr. Soc. Japan*, 47, 561

Takahashi, K. 1996, *Publ. Astr. Soc. Japan*, 48, 691

Takahashi, K., Lee, H. M., Inagaki, S. 1997, *MNRAS*, 292, 31